Biochimica et Biophysica Acta 1793 (2009) 273–280

Contents lists available at ScienceDirect

Biochimica et Biophysica Acta

journal homepage: www.elsevier.com/locate/bbamcr

Intracellular zinc increase inhibits p53$^{-/-}$ pancreatic adenocarcinoma cell growth by ROS/AIF-mediated apoptosis

M. Donadelli [a], E. Dalla Pozza [a], M.T. Scupoli [b], C. Costanzo [a], A. Scarpa [c], M. Palmieri [a,*]

[a] Department of Morphological and Biomedical Sciences, Section of Biochemistry, University of Verona, Strada Le Grazie, 8, 37134 Verona, Italy
[b] Interdepartmental Laboratory for Medical Research (LURM), University of Verona, Italy
[c] Department of Pathology, Section of Anatomic Pathology, University of Verona, Italy

ARTICLE INFO

Article history:
Received 7 March 2008
Received in revised form 15 September 2008
Accepted 15 September 2008
Available online 7 October 2008

Keywords:
Pancreatic adenocarcinoma
Zinc
Pyrrolidine dithiocarbamate
Oxidative stress
p53

ABSTRACT

We show that treatment with non-toxic doses of zinc in association to the ionophore compound pyrrolidine dithiocarbamate (PDTC) inhibits p53$^{-/-}$ pancreatic cancer cell growth much more efficiently than gemcitabine, the gold standard chemotherapeutic agent for pancreatic cancer. Both the metal chelator *N*,*N*,*N*′,*N*′-tetrakis(2-pyridylmethyl)ethylenediamine and the radical scavenger *N*-acetyl-L-cysteine are able to recover cell growth inhibition by Zn/PDTC, demonstrating that this effect depends on the increased levels of intracellular zinc and of reactive oxygen species (ROS). Zn/PDTC treatment induces a strong apoptotic cell death that is associated to ROS-dependent nuclear translocation of the mitochondrial factor AIF, but not to the regulation of apoptotic genes and caspase activation. Primary fibroblasts are more resistant than pancreatic cancer cells to Zn/PDTC treatment and exhibit a lower basal and Zn/PDTC-induced enhancement of intracellular zinc. We show that Zn/PDTC induces p53 proteasomal degradation and that the proteasome inhibitor MG132 further increases fibroblast growth inhibition by Zn/PDTC, suggesting that p53 degradation plays an important role in fibroblast resistance to Zn/PDTC.

1. Introduction

Pancreatic cancer is characterized by high frequency mutations in *TP53*, *K-RAS*, *P16*, and *DPC4* genes [1]. Despite advances in the understanding of the molecular biology, prognosis of this cancer remains dismal with a 5-year survival of less than 5% [2] and the gold standard chemotherapy with gemcitabine is largely ineffective [3].

Zinc is an important modulator of various cellular activities with both catalytic and structural roles [4]. It is the cofactor of over 300 enzymes and is involved in the stabilization of the three-dimensional structure of many proteins, including more than 100 transcription factors containing zinc finger domains [5]. Owing to these critical roles, the cellular homeostasis of zinc ions is strictly controlled at different levels by cell membrane zinc transporters [6], metallothionein sequestration [7], and storing in intracellular compartments called "zincosomes" [8]. Although zinc is an essential element, its excess induces apoptosis in different cell lines involving mitochondrial injury and oxidative stress production [9,10].

Growing evidence indicates that cancer cells exhibit an intrinsic oxidative stress higher than normal cells [11,12]. Thus, exposure to further ROS insults is likely to cause more injury in cancer than in normal cells because of a more rapid exhaustion of the antioxidant defences [11]. In line with this observation, it has been found that free radical production is one of the means by which many anticancer agents and ionizing radiation exert their killing effect [12].

Here, we report that zinc-mediated ROS increase, obtained by treating cells with zinc in association to the ionophore pyrrolidine dithiocarbamate (PDTC), is a strong inhibitor of pancreatic cancer cell growth, whereas it is much less efficient on normal primary fibroblasts. Zn/PDTC has a higher activity than gemcitabine and induces caspase-independent apoptosis that is associated to the nuclear translocation of the mitochondrial apoptosis inducing factor (AIF). Furthermore, our data indicate that the resistance of normal primary fibroblasts to Zn/PDTC treatment most likely depends on i) a lower basal level and Zn/PDTC-mediated increase of intracellular zinc compared to pancreatic cancer cells and ii) p53 degradation by Zn/PDTC-mediated proteasome activation.

2. Materials and methods

2.1. Chemicals

Pyrrolidine dithiocarbamate (PDTC), *N*-acetyl-L-cysteine (NAC), zinc sulfate (Sigma) and gemcitabine (GEM; Gemzar, Lilly) were freshly prepared in sterile water. *N*,*N*,*N*′,*N*′-tetrakis(2-pyridylmethyl)

* Corresponding author. Tel.: +39 045 8027169; fax: +39 045 8027170.
E-mail address: marta.palmieri@univr.it (M. Palmieri).

0167-4889/$ – see front matter © 2008 Elsevier B.V. All rights reserved.
doi:10.1016/j.bbamcr.2008.09.010

ethylenediamine (TPEN; Sigma) was prepared in absolute ethanol and stored at −80 °C until use. The broad spectrum caspase inhibitor Z-VAD-FMK and the proteasome inhibitor MG132 (Biomol) were prepared in DMSO and stored at −80 °C until use.

2.2. Cell culture

Four human pancreatic adenocarcinoma cell lines were studied: PaCa44, T3M4, Panc1, and CFPAC1 [see [1] for genetic characterization and primary tissue source]. All cell lines were grown in RPMI 1640 supplemented with 20 mM glutamine, 10% FBS and 50 μg/ml gentamicin sulfate (BioWhittaker) and were incubated at 37 °C with 5% CO_2. Primary fibroblasts were grown in DMEM supplemented with 20 mM glutamine, 10% FBS and 50 μg/ml gentamicin sulfate and were incubated at 37 °C with 5% CO_2.

2.3. Cell proliferation assay

Cells were plated in 96-well plates (4×10^3 cells/well) and 24 h later were treated with the appropriate compounds (see figure legends) and further incubated for 6 or 24 h; then cells were stained with crystal violet (Sigma). The dye was solubilised in PBS containing 1% SDS and measured photometrically ($A_{595\ nm}$) to determine cell viability. At the concentrations used in this work, $ZnSO_4$ remained soluble in 10% FBS containing media, which were the same as those used for growing cells.

2.4. Apoptosis

The percentage of apoptotic cells was evaluated by staining 2×10^5 cells with annexin V-FITC (Bender Med System) and 5 mg/ml propidium iodide in binding buffer [10 mM HEPES/NaOH (pH 7.4), 140 mM NaOH, and 2.5 mM $CaCl_2$] for 10 min at room temperature in the dark. The samples were analyzed by flow cytometry (FACScalibur, Becton-Dickinson) to determine the percentage of cells displaying annexin V^+/propidium $iodide^-$ (early apoptosis) or annexin V^+/propidium $iodide^+$ staining (late apoptosis).

Caspase 3 and caspase 8 activities were assayed by cleavage of the fluorogenic substrates Ac-DEVD-AMC and Ac-IETD-AMC (Biomol), respectively. After the indicated treatments, cells were washed twice with ice-cold PBS and lysed in caspase buffer (100 mM HEPES, 200 mM NaCl, 1 mM EDTA, 20 mM CHAPS, 10% sucrose). Lysates were prepared by repeated freeze-thawing, centrifuged at 14,000 ×*g* for 10 min and the supernatant fraction saved for analysis. 100 μg of total protein extract were incubated with 10 μg of the fluorogenic peptide substrates in a total volume of 800 μl. After a 10 min (caspase 3) or 20 min (caspase 8) incubation at 30 °C, the release of 7-amino-4-methylcoumarin was determined fluorometrically (excitation wavelength of 380 nm; emission wavelength of 460 nm). Optimal amounts of cell lysate and duration of assay were determined in preliminary experiments.

2.5. Analysis of the intracellular zinc level

Cells (2×10^5) were stained with 2 μM FluoZin-3 (Molecular Probes) at 37 °C for 30 min, washed in probe-free medium to remove any dye that is nonspecifically associated and further incubated for 10 min at 37 °C to allow complete intracellular de-esterification of the probe. Afterwards, cells were washed twice in PBS and analyzed by flow cytometry (Ex/Em 494/516 nm).

2.6. Analysis of mitochondrial membrane potential ($\Delta\Psi m$)

Cells (2×10^5) were stained with 40 nM 3,3-dihexyloxacarbocyanine (Molecular Probes) at 37 °C for 20 min and washed twice in PBS. The percentage of cells exhibiting a decreased level of 3,3-dihexyloxacarbocyanine uptake, which reflects loss of $\Delta\Psi m$, was determined by flow cytometry.

2.7. RNA extraction, RT-PCR, and image analysis

Total RNA was extracted from 5×10^6 cells using TRIzol Reagent (Invitrogen) and 1 μg of RNA was reverse transcribed using First Strand cDNA Synthesis for RT-PCR (Invitrogen). For each sample, one tenth of the cDNA was used as a template for PCR amplification using the following primers and cycling conditions: β-actinFor 5′-ACCAACTGGGACGACATGGAGAA-3′ and β-actinRev 5′-GTGGTGGTGAAGCTGTAGCC-3′, 25 cycles of 94 °C for 60 s, 55 °C for 60 s and 72 °C for 60s; Bcl-xLFor/Bcl-xSFor 5′-CGGGCATTCAGTGACCTGAC-3′ and Bcl-xLRev/Bcl-xSRev 5′-TCAGGAACCAGCGGTTGAAG-3′, 35 cycles of 94 °C for 30 s, 50 °C for 30 s and 72 °C for 30 s; Bcl-wFor 5′-AAGCTGAGGCAGAAGGGTTA-3′ and Bcl-wRev 5′-CCCAAAGACAAAGAAGGCTA-3′, 28 cycles of 94 °C for 30 s, 60 °C for 30 s and 72 °C for 30 s; Bcl-2For 5′-TGCACCTGACGCCCTTCAC-3′ and Bcl-2Rev 5′-AGACAGCCAGGAGAAATCAAACAG-3′, BaxFor 5′-ACCAAGAAGCTGAGCGAGTGTC-3′ and BaxRev 5′-ACAAAGATGGTCACGGTCTGCC-3′, BakFor 5′-TGAAAAATGGCTTCGGGGCAAGGC-3′ and BakRev 5′-TCATGATTTGAAGAATCTTCGTACC-3′, NoxaFor 5′-TGTCCGAGGTGCTCCAGTTG-3′ and NoxaRev 5′-TGCACCTTCACATTCCTCTC-3′, p53For 5′-CTGTGACTTGCACGTACTCC-3′ and p53Rev 5′-CCATGCAGGAACTGTTACAC-3′, 30 cycles of 94 °C for 30 s, 55 °C for 30 s and 72 °C for 30 s. PCR products were separated by electrophoresis through ethidium bromide-stained 2.0% agarose gel and visualized by ultraviolet light.

2.8. Measurement of reactive oxygen species (ROS) production

The non-fluorescent 2′,7′-dichlorofluorescin diacetate (DCF) probe, which becomes highly fluorescent on reaction with ROS, was used to evaluate cellular ROS production. Briefly, 2×10^5 cells were incubated with 10 μM DCF (Sigma) at 37 °C for 15 min and then analyzed by flow cytometry.

2.9. Immunocytochemistry

Cells ($3–5\times10^5$) were grown on coverslips and treated as indicated. Cells were washed twice in PBS, then fixed with 4% paraformaldehyde in PBS at room temperature for 30 min and permeabilised with acetone at −20 °C for 3 min. Coverslips were washed twice in PBS, incubated for 10 min with blocking solution (5% BSA in PBS) and probed with rabbit anti-human AIF antibody, (1:100 in blocking solution; Chemicon International) at room temperature for 1 h. Cells were subsequently washed three times in PBS and incubated with Alexa Fluor 488 anti-rabbit IgG antibody (1:200 in blocking solution; Invitrogen) in the dark at room temperature for 1 h. To assess nuclear morphology, cells were incubated with 4′,6-diamidino-2-phenylindole (DAPI) (1 μg/ml, Invitrogen) in the dark at room temperature for 8 min. Finally, cells were washed three times in PBS and mounted with 100% glycerol. Fluorescence was visualized using excitation/emission wavelengths of 488/520 nm (green) and 350/460 nm (blue) for AIF and DAPI, respectively. Cells were examined using a Canon fluorescence microscope with a 40× magnification.

2.10. Immunoblot analysis

Cells were collected, washed in phosphate-buffered saline, and resuspended in 20 mM Hepes pH 7.9, 0.4 M NaCl, 1 mM EDTA, 1 mM EGTA, 1 mM NaF, 1 mM Na_3VO_4, and 1× protease inhibitor cocktail (Roche). After three freeze/thaw cycles, the lysate was centrifuged at 14,000 ×*g* for 10 min at 4 °C and the supernatant was used for Western blot analysis. Protein concentration was measured with the Bradford protein assay reagent (Pierce) using bovine serum albumin as a standard. Fifty micrograms of protein extracts were electrophoresed through a 12% SDS-polyacrylamide gel and electro-blotted onto PVDF membranes (Millipore, Italy). Membranes were then incubated overnight at 4 °C with blocking solution [5% low-fat milk in TBST (100 mM

Tris, pH 7.5, 0.9% NaCl, 0.1% Tween 20)] and probed for 1 h at room temperature with the primary antibody anti-human phospho-p53 (Ser15) (1:1500 in blocking solution, Cell Signaling Technology) or anti-human p53 (1:500 in blocking solution, Santa Cruz Biotechnology). Horseradish peroxidase conjugated anti-mouse IgG (1:1000 in blocking solution, Upstate Biotechnology) was used to detect specific proteins. Immunodetection was carried out using the ECL chemiluminescent substrates (Amersham Pharmacia Biotech) and recorded using a HyperfilmECL (Amersham Pharmacia Biotech).

2.11. Statistical analysis

ANOVA (post hoc Bonferroni) analysis and graphical presentations were performed by GraphPad Prism version 5. p values less than 0.05, 0.01 or 0.001 were indicated as *, ** or ***, respectively.

3. Results

3.1. Zn/PDTC treatment strongly inhibits pancreatic adenocarcinoma cell growth

The antiproliferative effect of zinc was analyzed by treating PaCa44, CFPAC1, Panc1, and T3M4 pancreatic adenocarcinoma cell lines and normal primary fibroblasts with increasing doses of zinc ions. Fig. 1a shows that zinc determined a dose-dependent growth inhibition in all cell lines. This effect was considerably less intense in fibroblasts.

To test whether PDTC may enhance the cytotoxic effect of zinc, we first measured the zinc uptake by cells treated with 250 μM PDTC in the absence or presence of a non-toxic dose of zinc (10 μM, see Fig. 1a). Fig. 1b shows that the basal level of the intracellular zinc was 8-fold

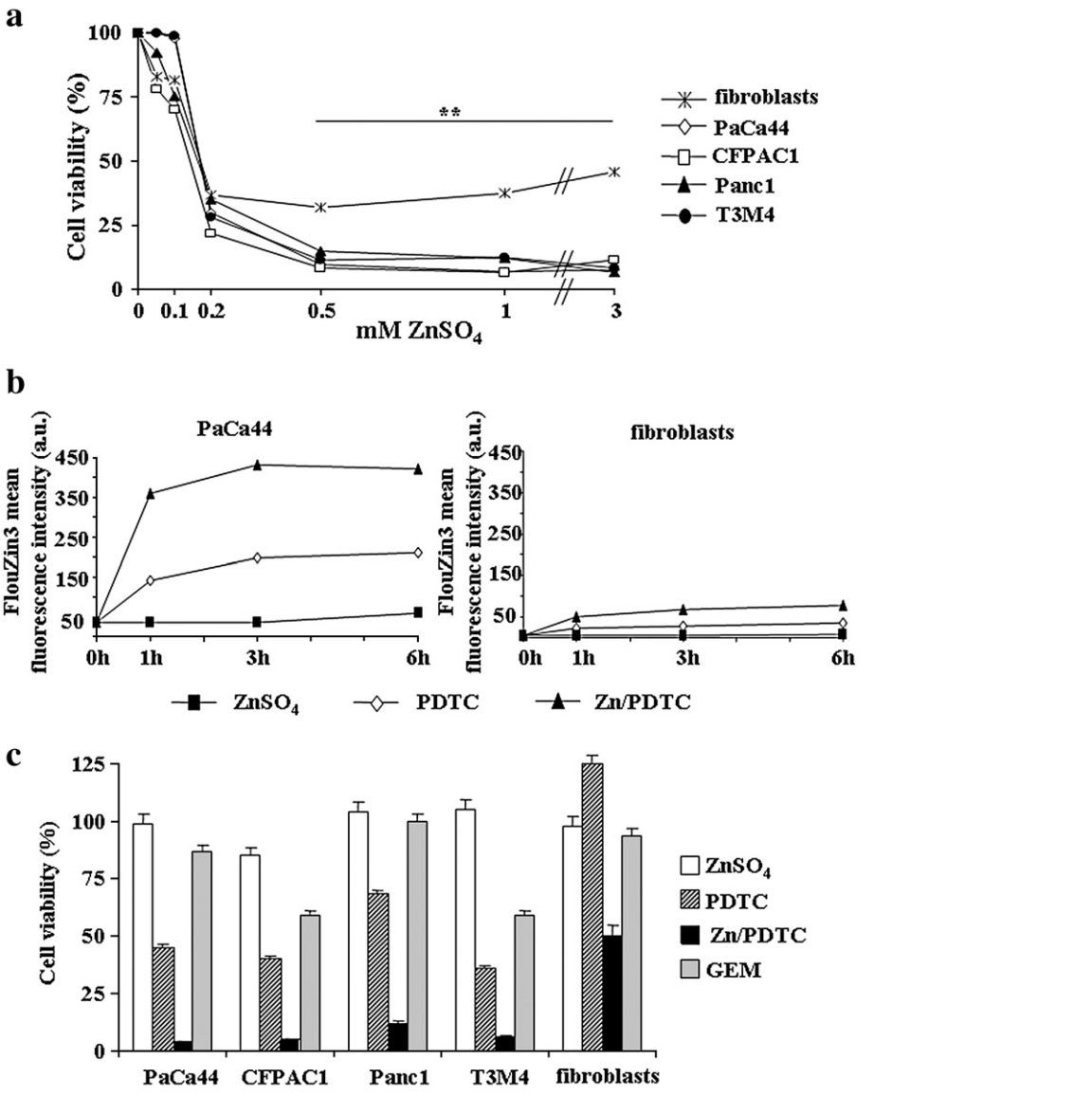

Fig. 1. Zn/PDTC treatment increases intracellular zinc level and inhibits pancreatic adenocarcinoma cell growth more efficiently than normal fibroblasts. (a) Four pancreatic adenocarcinoma cell lines (PaCa44, CFPAC1, Panc1, T3M4) and normal primary fibroblasts were treated with increasing doses of $ZnSO_4$ for 24 h. Cell proliferation was determined using the crystal violet colorimetric assay as described in Materials and methods. Values are the means of triplicate wells from three independent experiments. $^{**}p<0.01$ (fibroblasts versus pancreatic cell lines). (b) PaCa44 cells and normal primary fibroblasts were treated for the indicated time points with 10 μM $ZnSO_4$ (■), 250 μM PDTC (◊), or their association (▲). The FlouZin3 fluorescence intensity, corresponding to the intracellular zinc level, was measured by flow cytometry in arbitrary units (a.u.), as described in Materials and methods. Values are the means of three independent experiments. $^{***}p<0.001$ (PDTC or Zn/PDTC versus $ZnSO_4$, Zn/PDTC versus PDTC both in PaCa44 cells and fibroblasts) (c) Four pancreatic cancer cell lines (PaCa44, CFPAC1, Panc1, T3M4) and normal primary fibroblasts were treated with 10 μM $ZnSO_4$ and/or 250 μM PDTC, or 2 μM gemcitabine (GEM) for 24 h. Cell proliferation was determined using the crystal violet colorimetric assay. Values are the means of triplicate wells from three independent experiments (±SD). $^{***}p<0.001$ (Zn/PDTC versus $ZnSO_4$ or PDTC or GEM in all cells; Zn/PDTC in tumoural cells versus Zn/PDTC in fibroblasts).

lower in fibroblasts than in PaCa44 cells. Zn/PDTC treatment increased zinc uptake of about 12-fold both in fibroblasts and PaCa44 cells. As expected, also PDTC alone increased the intracellular zinc level, most likely by transferring into the cells zinc ions present in the culture medium. Fig. 1c shows that the exposure of cells to 10 μM zinc and 250 μM PDTC resulted in a stronger growth inhibition compared to PDTC alone. Noteworthy, Zn/PDTC treatment inhibited cell proliferation much more efficiently than gemcitabine (GEM), the gold standard chemotherapeutic agent for pancreatic cancer, and was much more efficient on pancreatic tumour cell lines than on normal fibroblasts (Fig. 1c). All together these data indicate that zinc-based treatment may be considered a novel efficient strategy to selectively inhibit pancreatic cancer cell growth.

3.2. The antiproliferative effect of Zn/PDTC is due to ROS-dependent apoptotic cell death

Fig. 2 shows that cell growth inhibition by Zn/PDTC treatment, analyzed at 6 h for PaCa44 cells and 24 h for fibroblasts, was recovered by the metal chelator TPEN or by the free radical scavenger NAC. The same experiment performed on PaCa44 cells treated for 24 h did not allow TPEN or NAC to completely recover cell viability inhibited by Zn/PDTC (Supplementary Fig. 1). On the other hand, fibroblasts were completely resistant to a 6 h treatment with Zn/PDTC (data not shown). Fig. 3a reports that Zn/PDTC determined a 5.5-fold ROS increase and that ROS production was totally abrogated by the addition of TPEN or NAC. As shown in Fig. 3b, TPEN was able to completely abrogate the zinc increase determined by Zn/PDTC treatment of cells, while NAC only partially decreased intracellular zinc in a dose dependent manner.

Flow cytometric analysis with annexin V-FITC and propidium iodide staining showed that treatment with Zn/PDTC induced a massive apoptotic cell death of PaCa44 cells (Fig. 3c), which was not observed after treatment with PDTC or zinc alone and was totally prevented by TPEN or by NAC at all concentrations tested, both at 6 h (see Fig. 3c) and 24 h (data not shown). This result and that shown in Fig. 3b indicate that NAC was protective even though Zn/PDTC was still taken up into the cells. Altogether, our results strongly suggest that the apoptotic event is dependent on the intracellular zinc increase and on the consequent ROS production. Consistent with the flow cytometric analysis, Zn/PDTC induced the release of nucleosomes in the cytoplasmic fraction of the cells, indicating the occurrence of apoptotic DNA cleavage (data not shown).

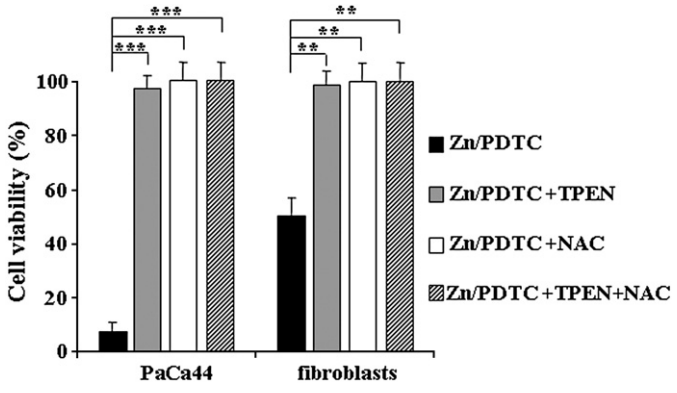

Fig. 2. NAC or TPEN recovers cell growth inhibition by Zn/PDTC treatment. PaCa44 cells and normal primary fibroblasts were treated with 250 μM PDTC and 10 μM $ZnSO_4$ in the absence or presence of 10 μM TPEN and/or 20 mM NAC for 6 h (PaCa44 cells) and 24 h (fibroblasts). Cell proliferation was determined using the crystal violet colorimetric assay. Values are the means of triplicate wells from three independent experiments (±SD). ***$p<0.001$, **$p<0.01$.

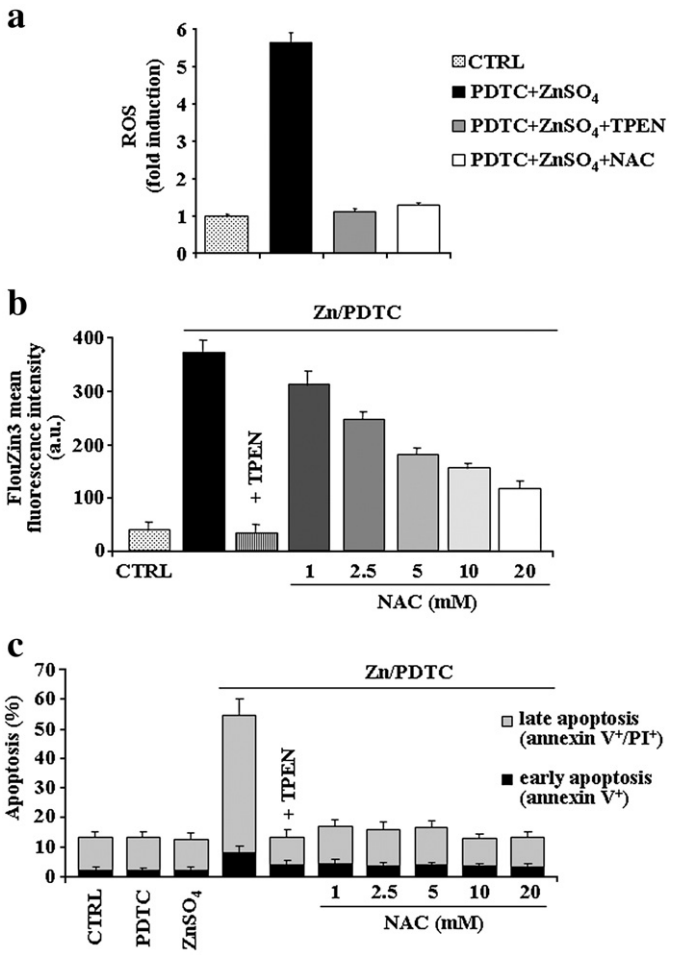

Fig. 3. Zn/PDTC treatment strongly induces ROS-dependent apoptosis. (a) PaCa44 cells were treated with 250 μM PDTC and 10 μM $ZnSO_4$ in the absence or presence of 10 μM TPEN or 20 mM NAC for 6 h. The 2′,7′-dichlorofluorescin (DCF) fluorescence intensity, corresponding to ROS production level, was measured by flow cytometry as described in Materials and methods. Values are the means of three independent experiments (±SD). (b) PaCa44 cells were treated for 6 h with 10 μM $ZnSO_4$ and 250 μM PDTC in the absence or presence of 10 μM TPEN or increasing concentrations of NAC. The FlouZin3 fluorescence intensity, corresponding to the intracellular zinc level, was measured by flow cytometry in arbitrary units (a.u.), as described in Materials and methods. Values are the means of three independent experiments (±SD). (c) PaCa44 cells were treated with 250 μM PDTC and/or 10 μM $ZnSO_4$ in the absence or presence of 10 μM TPEN or increasing concentrations of NAC for 6 h. 2×10^5 cells were analyzed by flow cytometry to determine the percentage of cells displaying annexin V^+/propidium $iodide^-$ (early apoptosis) or annexin V^+/ propidium $iodide^+$ staining (late apoptosis). The values are the means of three independent experiments (±SD).

3.3. Zn/PDTC determines ROS-dependent mitochondrial damage without activating caspases

It has been demonstrated that the production of ROS can increase mitochondrial membrane permeability, thus promoting the mitochondrion-mediated cell death program [13]. To determine whether mitochondria were involved in the apoptosis induced by Zn/PDTC, we measured the percentage of cells presenting a reduced mitochondrial membrane potential ($\Delta\Psi m$). In agreement with the apoptotic analyses (see Fig. 3c), either zinc or PDTC alone did not increase the percentage of cells with reduced $\Delta\Psi m$ compared with control, whereas the exposure to Zn/PDTC led to a reduction of $\Delta\Psi m$ in more than 50% of the cells (Fig. 4a). Moreover, TPEN or NAC addition totally prevented mitochondrial damage, demonstrating that this event depends on zinc intracellular increase and ROS production. Fig. 4b shows that zinc and/or PDTC treatments did not regulate the expression levels of some of the most

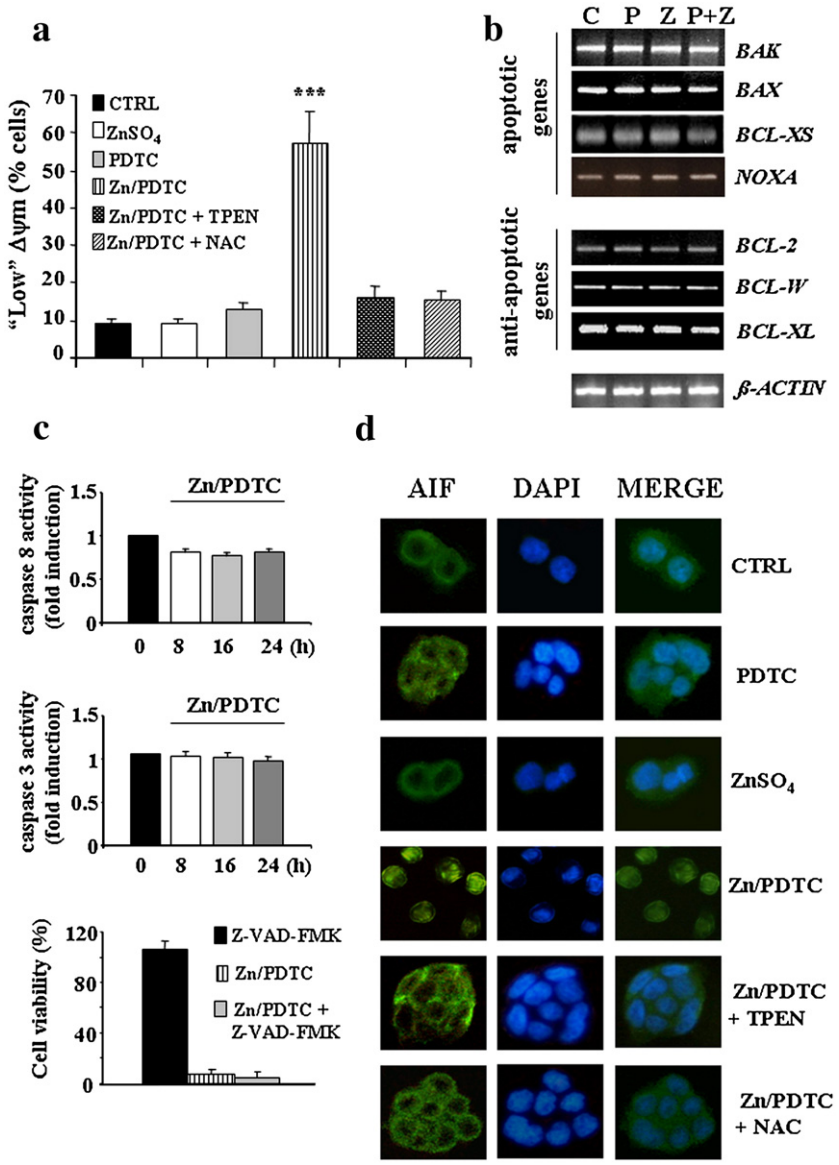

Fig. 4. Zn/PDTC treatment determines ROS-dependent mitochondrial damage and nuclear translocation of AIF. (a) PaCa44 cells were treated with 250 μM PDTC and/or 10 μM $ZnSO_4$ in the absence or presence of 10 μM TPEN or 20 mM NAC for 24 h. The percentage of cells exhibiting a reduced ΔΨm was determined by flow cytometry using 3,3-dihexyloxacarbocyanine staining as described in Materials and methods. Values are the means of three independent experiments (±SD). ***$p<0.001$. (b) RT-PCR analysis of the apoptotic and anti-apoptotic genes has been performed on total RNA obtained from PaCa44 cells treated with 250 μM PDTC and/or 10 μM $ZnSO_4$ for 8 h. Primer sequences and PCR conditions are described in Materials and methods. The results shown are representative of three independent experiments. The same results were obtained with incubation times of 16 and 24 h. (c) PaCa44 cells were exposed to 250 μM PDTC and 10 μM $ZnSO_4$ for the indicated time. Caspase 3 and 8 activities were assessed as described in Materials and methods. PaCa44 cells were treated with 250 μM PDTC and 10 μM $ZnSO_4$ and/or 100 μM Z-VAD-FMK, a pan caspase inhibitor, for 24 h. Cell proliferation was determined using the crystal violet colorimetric assay. Values are the means of triplicate wells from three independent experiments (±SD). (d) PaCa44 cells were treated with 250 μM PDTC and/or 10 μM $ZnSO_4$ in the absence or presence of 10 μM TPEN or 20 mM NAC for 24 h. AIF immunoreactivity (green) appeared within cell nuclei (labelled blue with DAPI) only in cells exposed to PDTC and zinc ions. The results shown are representative of three independent experiments.

important apoptotic (*BAK*, *BAX*, *BCL-XS*, and *NOXA*) and anti-apoptotic (*BCL-2*, *BCL-W*, and *BCL*-XL) genes, which are well known to promote or inhibit mitochondrial membrane damage, respectively.

Caspase activity assays demonstrated that both caspase 3 and caspase 8 were not activated following Zn/PDTC treatment and that the pan caspase inhibitor Z-VAD-FMK was not able to recover cell death by Zn/PDTC (Fig. 4c).

3.4. Zn/PDTC-induced apoptosis is associated to ROS-dependent nuclear translocation of AIF

Fig. 4d shows that treatment with Zn/PDTC determined a virtually complete nuclear translocation of the mitochondrial apoptotic inducing factor (AIF), which was totally abolished by TPEN or NAC. In contrast, zinc or PDTC alone were not able to promote nuclear translocation of AIF, according to the lack of apoptosis (Fig. 3c) and mitochondrial damage (Fig. 4a). These results were confirmed by Western blot assays using nuclear protein extracts (data not shown). All these data suggest that zinc-dependent ROS burst is responsible for translocation of AIF and they strongly support the fundamental role of zinc-mediated ROS generation in pancreatic cancer apoptotic cell death induced by Zn/PDTC.

3.5. Zn/PDTC strongly inhibits p53 expression in normal primary fibroblasts

As shown in Fig. 1c, normal primary fibroblasts were significantly more resistant than cancer cells to Zn/PDTC treatment. However, also

in fibroblasts zinc increase and oxidative stress have a crucial role in the reduction of cell viability as demonstrated by the complete recovery of cell proliferation by TPEN or NAC (Fig. 2).

We have previously reported that p53 phosphorylation in Ser15 induced by PDTC can protect cells from oxidative stress via the activation of the antioxidant gene *SESN2* [14,15]. Here, we show that the association Zn/PDTC neither increased the level of p53-(Ser15)-phosphorylation induced by PDTC alone, nor regulated the expression of antioxidant (*SESN1*, *SESN2*, and *GPX1*) and apoptotic (*BAX*, *BAK* and *NOXA*) p53-target genes (Supplementary Fig. 1). Zn/PDTC, however, strongly reduced p53 level by Zn- and ROS-dependent mechanisms (Fig. 5a and Supplementary Fig. 2), without altering *TP53* mRNA expression (Fig. 5b).

3.6. The proteasome inhibitor MG132 further inhibits fibroblast cell growth by Zn/PDTC

To investigate whether the proteasome was involved in p53 inhibition and in the reduced sensitivity of normal cells to Zn/PDTC treatment, we treated fibroblasts with the proteasome inhibitor MG132. Fig. 6 shows that MG132 was able to recover p53 degradation by Zn/PDTC (Fig. 6a) and that increasing concentrations of MG132 in the presence of Zn/PDTC determined a dose-dependent growth reduction compared to Zn/PDTC (Fig. 6b). MG132 alone did not significantly alter cell viability (data not shown). Altogether these data suggest that p53 degradation is an important event in fibroblast protection from Zn/PDTC-induced cell death.

4. Discussion

We have recently demonstrated that the ionophore compound PDTC inhibits growth of p53-negative human pancreatic cancer cell lines, while it has no effect on primary fibroblasts. We have also reported that PDTC is able to transport zinc ions present in the medium into the cells inducing a modest oxidative stress that is responsible for S-phase cell cycle arrest, but not for apoptotic cell death [14].

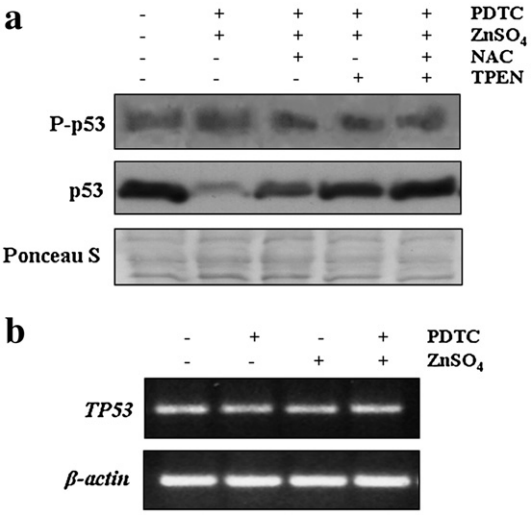

Fig. 5. Zn/PDTC treatment inhibits p53 expression in normal primary fibroblasts. (a) Western blot analysis of p53 and P(Ser15)-p53 was performed using total protein extracts from normal fibroblasts treated with 250 μM PDTC and 10 μM $ZnSO_4$ in the absence or presence of 10 μM TPEN and/or 20 mM NAC for 6 h. The same result was obtained with an incubation time of 16 h. (b) RT-PCR analysis of *TP53* mRNA was performed on total RNA obtained from normal fibroblasts treated with 250 μM PDTC and/or 10 μM $ZnSO_4$ for 6 h. Primer sequences and PCR conditions are described in Materials and methods. The results shown are representative of three independent experiments.

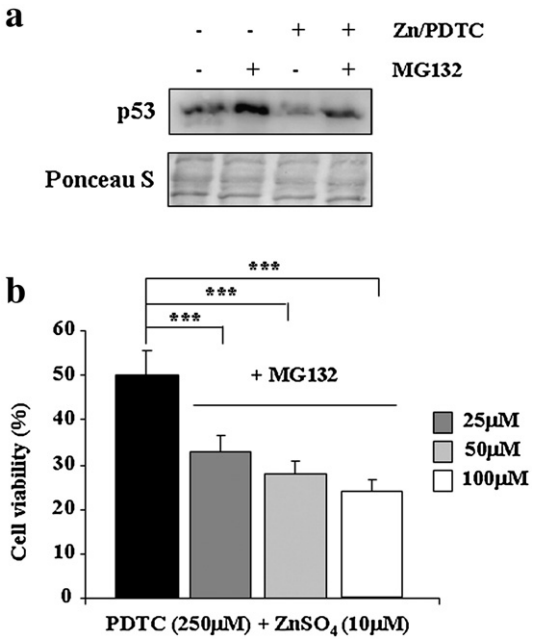

Fig. 6. The proteasome inhibitor MG132 further inhibits fibroblast cell growth by Zn/PDTC. (a) Western blot analysis of p53 was performed using total protein extracts from normal fibroblasts treated with 250 μM PDTC plus 10 μM $ZnSO_4$ and/or 100 μM MG132 for 6 h. The result shown is representative of three independent experiments. (b) Normal primary fibroblasts were treated with 250 μM PDTC plus 10 μM $ZnSO_4$ in the absence or presence of increasing concentrations of MG132 for 24 h. Cell growth was not significantly altered by treatment with MG132 alone (data not shown). Cell proliferation was determined using the crystal violet colorimetric assay. Values are the means of triplicate wells from three independent experiments (±SD). ***$p<0.001$.

We show here that a further increase of intracellular zinc, obtained by adding a non-toxic concentration of zinc to PDTC, induces on pancreatic cancer cells a much stronger ROS production (5.5-fold), as compared to PDTC alone (~2-fold). This event determines a strong apoptotic cell death, as suggested by the total recovery of viability after treatment with the metal chelator TPEN or the radical scavenger NAC. However, because of zinc binding activity of NAC, although very weak, we are unable to exclude that at least part of the apoptotic event depends directly on the intracellular zinc increase and not on the consequent ROS production. Anyway, the different trend of the two dose-dependent curves shown in Fig. 3b and c strongly suggests that the anti-apoptotic effect of NAC is not correlated with its chelating activity.

We report that the intracellular Zn/ROS increase generates a reduction of the mitochondrial membrane potential and the nuclear translocation of AIF, without affecting the expression of apoptotic and anti-apoptotic genes or caspase 3 and 8 activities. The analysis of the cell cycle shows that Zn/PDTC does not further induce pancreatic cancer cell cycle arrest in the S-phase by PDTC alone [14], indicating that the enhancement of cell growth inhibition by the addition of zinc to PDTC (Fig. 1c) is not caused by a stronger cytostatic effect (Supplementary Fig. 3).

In the last few years, it has been demonstrated that zinc ions are able to induce oxidative stress via quite different molecular mechanisms. They can stimulate ROS production by i) interacting with and inhibiting the mitochondrial complex III thus inducing mitochondrial respiration impairment [16,17]; ii) inhibiting glutathione reductase activity [18]; iii) inhibiting the lipoamide dehydrogenase multi-enzyme complex (LADH), which has a role in the preservation of the reducing environment of mitochondria [19].

Abnormally high levels of ROS have been demonstrated to trigger opening of mitochondrial permeability transition pores (mPTPs) and release into the cytosol of several different molecules that eventually

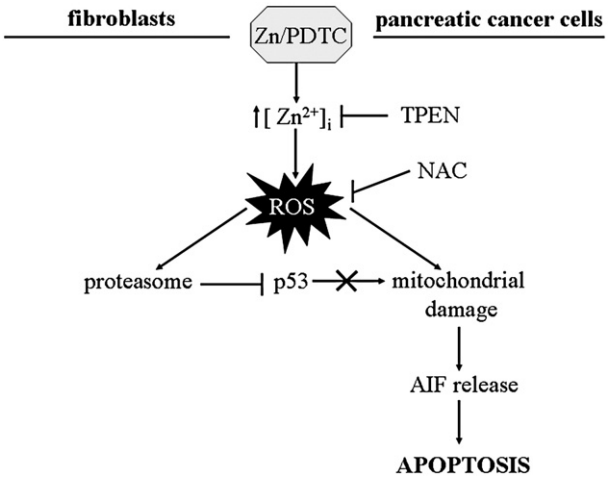

Fig. 7. Model of Zn/PDTC action. The molecular mechanisms identified in this study are shown. See text for further details.

lead to programmed cell death [13]. Our research group previously demonstrated that a modest induction of ROS by PDTC is capable of inducing p21-mediated cell cycle arrest in pancreatic cancer cells [14]. In the present manuscript, we show that a stronger increase of the ROS level determined by the association Zn/PDTC leads to a massive caspase-independent apoptosis associated to AIF release with no further increase of the cell cycle arrest. It has been demonstrated that mammalian cells can undergo apoptosis displaying a large-scale DNA fragmentation, which is uncoupled from caspase activation [20,21] and is dependent on AIF nuclear translocation [20]. In agreement with these observations, the apoptosis induced by Zn/PDTC treatment produces a large-scale DNA fragmentation that is not associated to the release of cytochrome *c* (data not shown). Altogether these data suggest that AIF may be the major effector of Zn/PDTC-induced apoptosis in pancreatic cancer cells.

Compared to pancreatic cancer cells, normal fibroblasts are less sensitive to Zn/PDTC treatment. Previously, we have reported that fibroblasts are totally resistant to the cytotoxic action of PDTC alone. This protective effect is most likely dependent on the activation of p53, via Ser 15 phosphorylation, and of p53-dependent antioxidant genes, which prevent the oxidative stress [14]. Here, we report that Zn/PDTC is able to inhibit fibroblast cell growth, although at a lower extent than pancreatic cells, by oxidative stress induction, as demonstrated by the total abrogation of the cytotoxic effect in the presence of NAC. Consistent with these results, the amount of Ser15-phosphorylated p53 remains unchanged following Zn/PDTC treatment as well as the levels of the antioxidant p53-target genes. Thus, a stronger oxidative stress determined by Zn/PDTC compared to PDTC alone, is neither able to activate p53 and its target antioxidant genes nor to totally protect cells from growth inhibition. However, fibroblasts appear more resistant than pancreatic adenocarcinoma cells to Zn/PDTC action. This effect correlates with the lower level of the intracellular zinc concentration following Zn/PDTC treatment in fibroblasts compared to pancreatic cancer cells.

Normal p53-wt cells, in contrast to p53-negative pancreatic adenocarcinoma cells, may activate the p53-mediated mechanisms of cell cycle arrest and/or apoptosis to counteract ROS induced DNA damage and its effects, thus further promoting cell growth inhibition. However, our data on normal fibroblasts demonstrate that Zn/PDTC treatment strongly reduces the level of p53 in a ROS-dependent manner, whereas either Ser15-phosphorylated p53 or p53 mRNA levels remain unchanged. Indeed, p53 inhibition by Zn/PDTC is due to enhanced degradation by the proteasome, as indicated by the abrogation of the effect in the presence of the proteasome inhibitor MG132. In addition, increasing concentrations of MG132 further inhibit fibroblast growth by Zn/PDTC, strongly suggesting that p53 degradation has an important role to prevent ROS-induced apoptosis in fibroblasts. It has recently been shown that besides its activity as a transcriptional regulator of apoptotic genes, p53 also exerts a direct pro-apoptotic role at the mitochondria [22]. Transcriptional functions of p53 require specific phosphorylations [23], whereas the direct apoptotic effect does not depend on p53 phosphorylation/acetylation [24]. Thus, our results suggest that the strong reduction of the p53 level determined by Zn/PDTC treatment of fibroblasts may decrease the contribution of the direct effect of p53 on apoptosis and protect cells from the cytotoxic effect of Zn/PDTC. Fig. 7 shows a model of the molecular mechanisms deduced from our data.

In cancer therapy, strategies are focused to reduce side effects that generally cause excessive apoptotic cell death in normal tissues. The aim is to develop small molecules that inhibit p53 to protect normal tissues from chemo- and radiotherapy [25]. Our demonstration that Zn/PDTC is able to strongly inhibit p53 expression in normal cells and is much more efficient than the gold standard gemcitabine in pancreatic cancer cell growth inhibition makes ROS increase by intracellular zinc enhancement a possible novel and efficient strategy for pancreatic cancer treatment.

Acknowledgments

This work was supported by Fondazione Cassa di Risparmio di Verona (Bando 2004); Associazione Italiana Ricerca sul Cancro, Milan, Italy. Italian Ministries of University–Research and Health; European Community grant PL PL018771; Fondazione Giorgio Zanotto, Verona, Italy.

Appendix A. Supplementary data

Supplementary data associated with this article can be found, in the online version, at doi:10.1016/j.bbamcr.2008.09.010.

References

[1] P.S. Moore, B. Sipos, S. Orlandini, C. Sorio, F.X. Real, N.R. Lemoine, T. Gress, C. Bassi, G. Kloppel, H. Kalthoff, H. Ungefroren, M. Lohr, A. Scarpa, Genetic profile of 22 pancreatic carcinoma cell lines. Analysis of K-ras, p53, p16 and DPC4/Smad4, Virchows Arch. 439 (2001) 798–802.
[2] D. Li, K. Xie, R. Wolff, J.L. Abbruzzese, Pancreatic cancer, Lancet 363 (2004) 1049–1057.
[3] D.G. Haller, New perspectives in the management of pancreas cancer, Semin. Oncol. 30 (2003) 3–10.
[4] K.A. McCall, C. Huang, C.A. Fierke, Function and mechanism of zinc metalloenzymes, J. Nutr. 130 (2000) 1437S–1446S.
[5] D. Beyersmann, H. Haase, Functions of zinc in signaling, proliferation and differentiation of mammalian cells, Biometals 14 (2001) 331–341.
[6] L.A. Gaither, D.J. Eide, Eukaryotic zinc transporters and their regulation, Biometals 14 (2001) 251–270.
[7] N. Saydam, T.K. Adams, F. Steiner, W. Schaffner, J.H. Freedman, Regulation of metallothionein transcription by the metal-responsive transcription factor MTF-1: identification of signal transduction cascades that control metal-inducible transcription, J. Biol. Chem. 277 (2002) 20438–20445.
[8] H. Haase, D. Beyersmann, Intracellular zinc distribution and transport in C6 rat glioma cells, Biochem. Biophys. Res. Commun. 296 (2002) 923–928.
[9] D. Jiang, P.G. Sullivan, S.L. Sensi, O. Steward, J.H. Weiss, Zn(2+) induces permeability transition pore opening and release of pro-apoptotic peptides from neuronal mitochondria, J. Biol. Chem. 276 (2001) 47524–47529.
[10] N. Schrantz, M.T. Auffredou, M.F. Bourgeade, L. Besnault, G. Leca, A. Vazquez, Zinc-mediated regulation of caspases activity: dose-dependent inhibition or activation of caspase-3 in the human Burkitt lymphoma B cells (Ramos), Cell Death Differ. 8 (2001) 152–161.
[11] A. Laurent, C. Nicco, C. Chereau, C. Goulvestre, J. Alexandre, A. Alves, E. Levy, F. Goldwasser, Y. Panis, O. Soubrane, B. Weill, F. Batteux, Controlling tumor growth by modulating endogenous production of reactive oxygen species, Cancer Res. 65 (2005) 948–956.
[12] H. Pelicano, D. Carney, P. Huang, ROS stress in cancer cells and therapeutic implications, Drug Resist. Updat. 7 (2004) 97–110.
[13] C. Fleury, B. Mignotte, J.L. Vayssiere, Mitochondrial reactive oxygen species in cell death signaling, Biochimie 84 (2002) 131–141.
[14] M. Donadelli, E. Dalla Pozza, C. Costanzo, M.T. Scupoli, P. Piacentini, A. Scarpa, M. Palmieri, Increased stability of P21(WAF1/CIP1) mRNA is required for ROS/ERK-dependent pancreatic adenocarcinoma cell growth inhibition by pyrrolidine dithiocarbamate, Biochim. Biophys. Acta 1763 (2006) 917–926.

[15] A.A. Sablina, A.V. Budanov, G.V. Ilyinskaya, L.S. Agapova, J.E. Kravchenko, P.M. Chumakov, The antioxidant function of the p53 tumor suppressor, Nat. Med. 11 (2005) 1306–1313.
[16] E.A. Berry, Z. Zhang, H.D. Bellamy, L. Huang, Crystallographic location of two Zn(2+)-binding sites in the avian cytochrome *bc*(1) complex, Biochim. Biophys. Acta 1459 (2000) 440–448.
[17] A.M. Brown, B.S. Kristal, M.S. Effron, A.I. Shestopalov, P.A. Ullucci, K.F. Sheu, J.P. Blass, A.J. Cooper, Zn2+ inhibits alpha-ketoglutarate-stimulated mitochondrial respiration and the isolated alpha-ketoglutarate dehydrogenase complex, J. Biol. Chem. 275 (2000) 13441–13447.
[18] G.M. Bishop, R. Dringen, S.R. Robinson, Zinc stimulates the production of toxic reactive oxygen species (ROS) and inhibits glutathione reductase in astrocytes, Free Radic. Biol. Med. 42 (2007) 1222–1230.
[19] I.G. Gazaryan, B.F. Krasnikov, G.A. Ashby, R.N. Thorneley, B.S. Kristal, A.M. Brown, Zinc is a potent inhibitor of thiol oxidoreductase activity and stimulates reactive oxygen species production by lipoamide dehydrogenase, J. Biol. Chem. 277 (2002) 10064–10072.
[20] X. Zhang, J. Chen, S.H. Graham, L. Du, P.M. Kochanek, R. Draviam, F. Guo, P.D. Nathaniel, C. Szabo, S.C. Watkins, R.S. Clark, Intranuclear localization of apoptosis-inducing factor (AIF) and large scale DNA fragmentation after traumatic brain injury in rats and in neuronal cultures exposed to peroxynitrite, J. Neurochem. 82 (2002) 181–191.
[21] N. Joza, S.A. Susin, E. Daugas, W.L. Stanford, S.K. Cho, C.Y. Li, T. Sasaki, A.J. Elia, H.Y. Cheng, L. Ravagnan, K.F. Ferri, N. Zamzami, A. Wakeham, R. Hakem, H. Yoshida, Y.Y. Kong, T.W. Mak, J.C. Zuniga-Pflucker, G. Kroemer, J.M. Penninger, Essential role of the mitochondrial apoptosis-inducing factor in programmed cell death, Nature 410 (2001) 549–554.
[22] U.M. Moll, N. Marchenko, X.K. Zhang, p53 and Nur77/TR3 — transcription factors that directly target mitochondria for cell death induction, Oncogene 25 (2006) 4725–4743.
[23] W.T. Steegenga, A.J. van der Eb, A.G. Jochemsen, How phosphorylation regulates the activity of p53, J. Mol. Biol. 263 (1996) 103–113.
[24] A. Nemajerova, S. Erster, U.M. Moll, The post-translational phosphorylation and acetylation modification profile is not the determining factor in targeting endogenous stress-induced p53 to mitochondria, Cell Death Differ. 12 (2005) 197–200.
[25] A.V. Gudkov, E.A. Komarova, Prospective therapeutic applications of p53 inhibitors, Biochem. Biophys. Res. Commun. 331 (2005) 726–736.